

## Parametrization of pion-nucleon phase shifts and effects upon pion-nucleus scattering calculations

A. A. Ebrahim\* and R. J. Peterson

*Nuclear Physics Laboratory, University of Colorado, Boulder, Colorado 80309-0446*

(Received 17 June 1996)

Pi meson interactions with free nucleons as known from recent experiments have been fit by Arndt *et al.* in the form of phase shifts. In the present work these phase shifts are fit by a simple parametrization, and observables computed from the resulting parametrized phase shifts are compared successfully to important examples of recent measurements. The parameters of this work are readily suited to pion-nucleus optical model codes built upon the impulse approximation. Some examples of the effect of the new pion-nucleon data upon these pion-nucleus calculations are shown, relative to older results based upon far fewer pion-nucleon data. [S0556-2813(96)00211-7]

PACS number(s): 25.80.Dj, 25.80.Ek, 25.80.Gn

### I. INTRODUCTION

Many pion-nucleus reaction models are built upon the impulse approximation, using the interaction of the mesons with free nucleons. Although there are several general compilations of those free space interactions, it has been convenient to use the parametrization and fitted results of Rowe, Salomon, and Landau [1] in pion-nucleus optical model codes, such as those of [2,3].

Rowe, Salomon, and Landau fit the  $\pi$ -nucleon data available in 1978, before the high intensity meson facilities were able to generate the large body of data now available. Especially at low pion beam energies, the newer data differ significantly from the data base used by Rowe, Salomon, and Landau. Since so many important conclusions have been drawn from  $\pi$ -nucleus interactions, and since many of those conclusions are based in some form upon the  $\pi$ -nucleon impulse approximation, it is important to reexamine those calculations using a modern base of  $\pi$ -nucleon interactions.

In this work we use the systematically fitted compilation of Arndt *et al.* [4] in their program SAID. The SM95 solution is used, since the data set used in this solution has been critically examined, and includes important new measurements with good statistical accuracy and with greatly improved understandings of systematic uncertainties. The researchers involved in these studies have produced a series of  $\pi$ - $N$  newsletters containing their results and their debates [5].

In Sec. II of this work the formulation of Rowe, Salomon, and Landau (RSL) is used to fit the  $\pi$ -nucleon phase shifts from the SM95 solution in SAID. The parametrization so obtained is then used to compute  $\pi$ -nucleon observables for comparison to a number of accurate and sensitive experiments and to observables calculated using the original RSL parameters. In Sec. III the results of using the new parametrization in optical model calculations in place of the older one of RSL for pions are compared to data for pion-nucleus

elastic, inelastic, and charge exchange scattering and to computations identical except for the use of the RSL parameters. If there were to be significant differences between calculations from the two parameter sets, an extensive reanalysis of the conclusions drawn from theoretical analyses of pion-nucleus scattering would be required. Section IV provides a summary of what effect the new  $\pi$ -nucleon data will have upon conclusions drawn from  $\pi$ -nucleus impulse approximation calculations.

### II. THE $\pi$ -NUCLEON INTERACTION

The  $\pi$ -nucleon phase shifts to be fit were obtained from the SM95 solution incorporated in the program SAID [4], from 30 to 300 MeV of laboratory-frame pion kinetic energy. This is the energy range most used for  $\pi$ -nucleus experiments, and the restriction to 300 MeV maintains the elasticity of the  $\pi$ -nucleon amplitudes. The phase shifts fitted are then purely real.

The form of the parametrization is exactly that of RSL, restricted to the partial waves listed in Table I. This form incorporates the threshold behavior expected on general grounds and the lowest resonance for each partial wave. All other  $\pi$ -nucleon phase shifts were set to zero. The form is

TABLE I. Resonance parameters for Eq. (1), using the lightest resonance for each partial wave. The resonance energy is  $\omega_0$ , its width is  $\Gamma$  and  $|r|$  is the absolute value of the residue. For Eq. (1) we use  $x=2|r|/\Gamma$  and  $q_0$  for the center of the mass momentum of the  $\pi$ - $N$  system to reach  $\omega_0$ . These values are from Ref. [6].

Channel	$x$	$\omega_0$ (MeV)	$q_0$ (MeV/c)	$\Gamma$ (MeV)	$ r $ (MeV)
S11	0.31	1535	464	150	23
S31	0.25	1620	527	150	19
P11	0.23	1440	482	350	40
P13	0.20	1720	594	150	15
P31	0.30	1910	717	250	38
P33	0.83	1232	228	120	50
D13	0.53	1520	457	120	32
D15	0.31	1675	566	150	23

\*Permanent address: Department of Physics, Assiut University, Assiut 71516, Egypt.

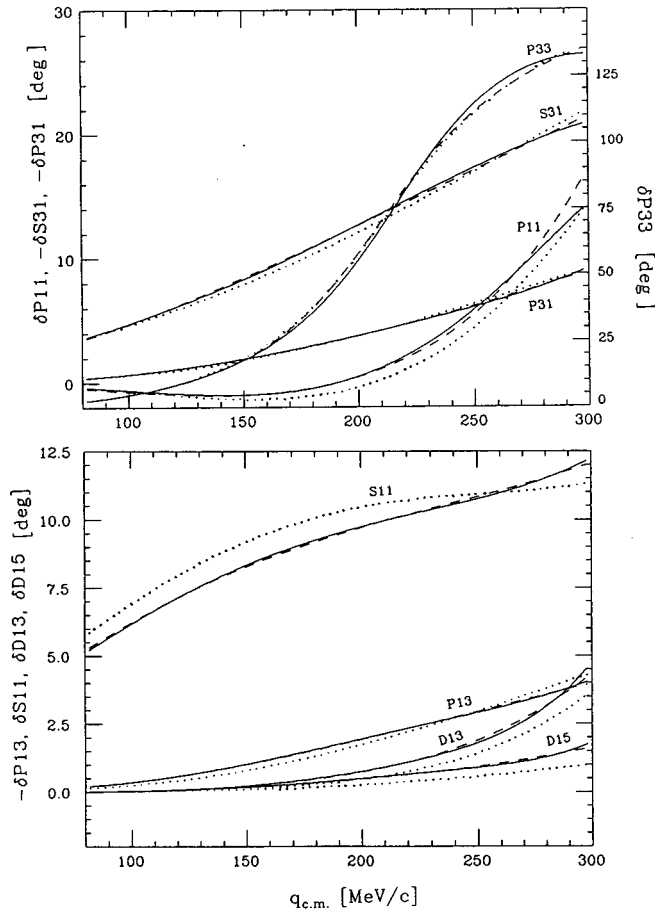


FIG. 1. Phase shifts for  $\pi$ -nucleon elastic scattering are shown for the partial waves considered in the present work. Dotted curves show the results using the RSL parametrization [1], the dashed curves show the phase shifts from the fitting in SAID for the SM95 solution [4], and the solid curves show the phase shifts computed from the parameters of the present work, as listed in Table I. These were obtained by fitting the SAID phase shifts with the parametrization form of RSL.

$$\frac{\tan \delta_{\ell}}{q^{2\ell+1}} = b + cq^2 + dq^4 + \frac{x\Gamma\omega_0q_0^{-(2\ell+1)}}{\omega_0^2 - \omega^2}. \quad (1)$$

The parameters for the resonances are listed in Table I, obtained from the most recent compilation [6]. These parameters are the location, width, and residue for each  $\pi$ -nucleon resonance, using the strength parameter  $x = 2|r|/\Gamma$ , where  $r$  is the residue of each pole.

In fitting the phase shifts from SAID the weight of each point was obtained using a uniform 10% uncertainty. Since no clearly established means of evaluating the uncertainties for  $\pi$ -nucleon phase shifts is agreed upon, this arbitrary value was used. In the results below, the uncertainties in the coefficients  $b$ ,  $c$ ,  $d$  can then only indicate the relative sensitivity of that coefficient to the phase shift. Starting parameters for  $b$ ,  $c$ , and  $d$  were taken to be the final results from RSL [1].

Table II lists the coefficients  $b$ ,  $c$ ,  $d$  obtained from fitting the phase shifts from SAID. Units of MeV/c are used. Figure 1 shows the resulting phase shifts from this param-

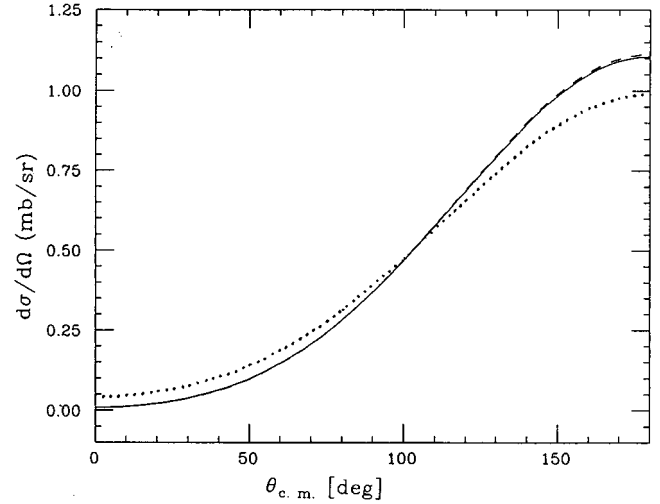


FIG. 2. Computed cross sections for  $\pi^-$ -proton charge exchange at 39.4 MeV are compared for the three phase shift sets used in this work. The dotted curve uses the RSL form, the dashed curve the SAID full solution, and the solid curve uses the parameters in Table I.

etrization, compared to those from SAID (to which we made a fit), and to those from the work of Rowe, Salomon, and Landau. The horizontal scale uses the center-of-mass momentum. Agreement between the present results and the SAID results fitted is very good, of course. In Fig. 1(a) the greatest difference from the RSL results is found for the  $P11$  wave. In Fig. 1(b) the  $S11$  wave from the work of RSL is significantly above the newer results at low momenta, while the small  $D$ -wave phase shifts differ above about 150 MeV/c. In general, the phase shifts based upon newer data differ remarkably little from those provided by RSL.

Since  $\pi$ -nucleon observables are generated by coherent combinations of amplitudes computed from these phase

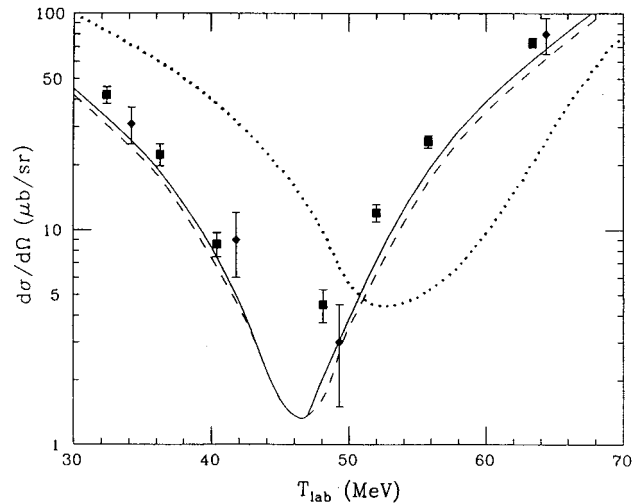


FIG. 3.  $0^\circ$  charge exchange differential cross sections are shown for the three phase shift sets used in the present work, with the meanings as in Fig. 1. Square data points show the  $\pi^-$ -proton data of Ref. [8], and diamond points show half the values found in the  $(\pi^+, \pi^0)$  reaction to the isobaric analog state of  $^{14}\text{C}$  [9].

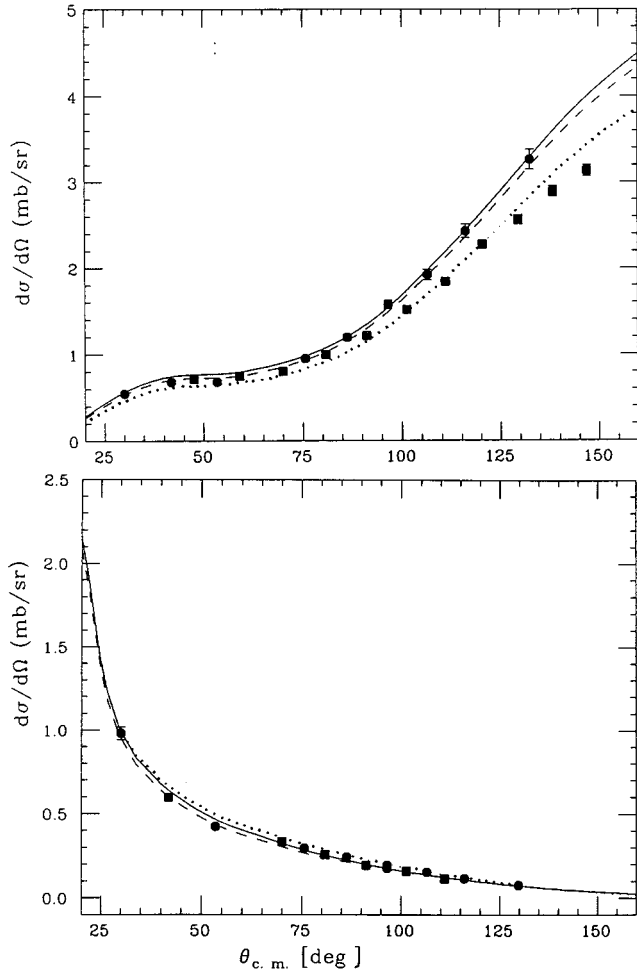


FIG. 4. Differential elastic cross sections at 68.6 MeV [10], shown as circles, are compared to calculations using the three phase shift forms considered in this work, with the same meanings for the curves as in Fig. 1. Positive pion results are shown above, and negative pion results are shown below. Also shown are square data points at 66.8 MeV [11].

shifts, there can be sensitivities not readily evaluated by examining only the phase shifts themselves. We have used the program SAID to compute  $\pi$ -nucleon observables using all three phase shift sets: SM95, RSL, and the present work. Examples are taken from a wide range of energies for 30–300 MeV, emphasizing observables particularly sensitive to interferences. Only the partial waves listed in Table I were used for the calculations with the parametrized phase shifts, while partial waves up to the  $I$  wave are used in the SAID computations.

Curves showing cross sections for pion charge exchange at 39.4 MeV computed with the three phase shift sets are shown in Fig. 2. These are almost indistinguishable for SAID and the present solutions, with the RSL values somewhat different. No data such as these were available to RSL, but new experimental results are very similar to the solid and dashed lines in Fig. 2 [7].

Another view of the isovector interaction is available from the  $0^\circ$  excitation function shown in Fig. 3. A distinctive minimum is found near 46 MeV, due to the destructive interference of the spin-independent isovector  $S$  and  $P$  am-

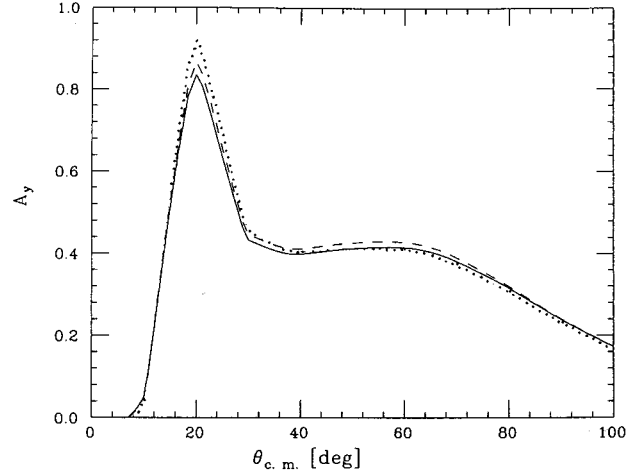


FIG. 5. The analyzing powers for elastic  $\pi^+$  proton elastic scattering at 68.34 MeV are compared for the phase shift forms of the present work, using the same meanings for the curves as Fig. 1.

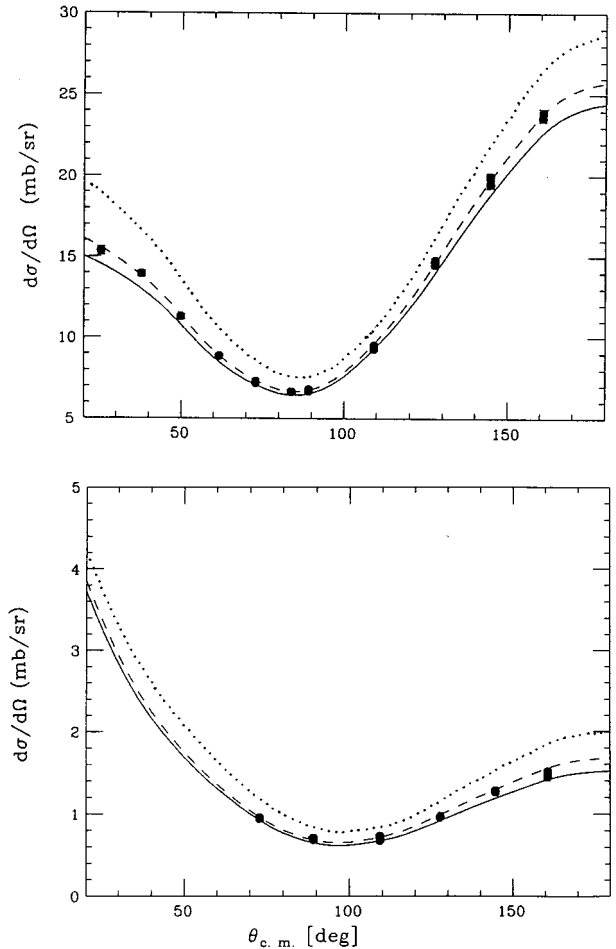


FIG. 6. Elastic differential cross sections at 141.15 MeV [12] are compared to curves showing the results of using the three phase shift forms of the present work, using the same meanings as found in Fig. 1. Positive pion results are shown above, and negative pion results are shown below.

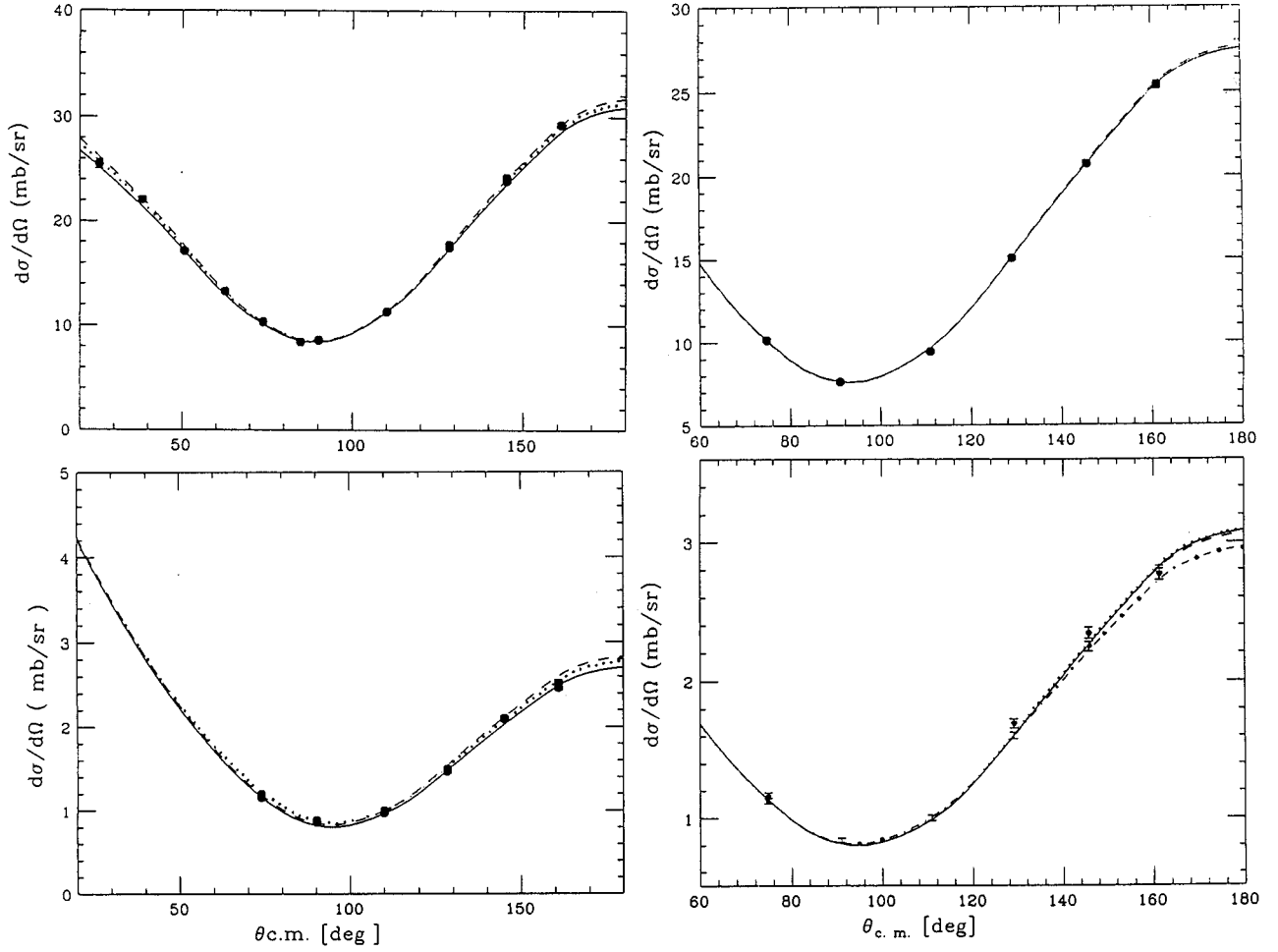


FIG. 7. Elastic differential cross sections atop the 3-3 resonance [12] are compared to curves showing the cross sections computed from the three phase shift forms considered in the present work. The meanings of the curves are as in Fig. 1. The left plots are for pion energies of 168.8 MeV and the right plots are for 193.15 MeV, with positive pion results above and negative pion results below.

TABLE II. Parameters  $b$ ,  $c$ ,  $d$  in powers of (MeV/c) for Eq. (1). The uncertainties (below the values) were obtained assuming a uniform 10% uncertainty in the phase shift being fit.

Channel	$b$	$c$	$d$
S11	$1.053099 \times 10^{-3}$	$-1.123708 \times 10^{-8}$	$5.366957 \times 10^{-14}$
	$4.3531 \times 10^{-6}$	$2.0621 \times 10^{-10}$	$2.0612 \times 10^{-15}$
S31	$-7.709957 \times 10^{-4}$	$-1.465965 \times 10^{-8}$	$8.485826 \times 10^{-14}$
	$6.8934 \times 10^{-6}$	$4.2083 \times 10^{-10}$	$4.7177 \times 10^{-15}$
P11	$-1.720423 \times 10^{-8}$	$5.382523 \times 10^{-13}$	$-3.055784 \times 10^{-18}$
	$5.3515 \times 10^{-10}$	$2.2919 \times 10^{-14}$	$2.3675 \times 10^{-19}$
P13	$-7.300847 \times 10^{-9}$	$9.093504 \times 10^{-14}$	$-4.633992 \times 10^{-19}$
	$5.1073 \times 10^{-11}$	$2.2270 \times 10^{-15}$	$2.1364 \times 10^{-20}$
P31	$-1.313602 \times 10^{-8}$	$1.481661 \times 10^{-13}$	$-7.853222 \times 10^{-19}$
	$1.0436 \times 10^{-10}$	$4.6739 \times 10^{-15}$	$4.5193 \times 10^{-20}$
P33	$4.810577 \times 10^{-8}$	$-2.268685 \times 10^{-13}$	$-1.291258 \times 10^{-18}$
	$2.4549 \times 10^{-9}$	$1.6299 \times 10^{-13}$	$1.5329 \times 10^{-18}$
D13	$7.714106 \times 10^{-14}$	$-1.444489 \times 10^{-18}$	$9.919875 \times 10^{-24}$
	$1.8386 \times 10^{-15}$	$8.0999 \times 10^{-20}$	$7.9589 \times 10^{-25}$
D15	$6.636850 \times 10^{-14}$	$-1.325509 \times 10^{-18}$	$8.011451 \times 10^{-24}$
	$4.9142 \times 10^{-15}$	$1.8248 \times 10^{-19}$	$1.5784 \times 10^{-24}$

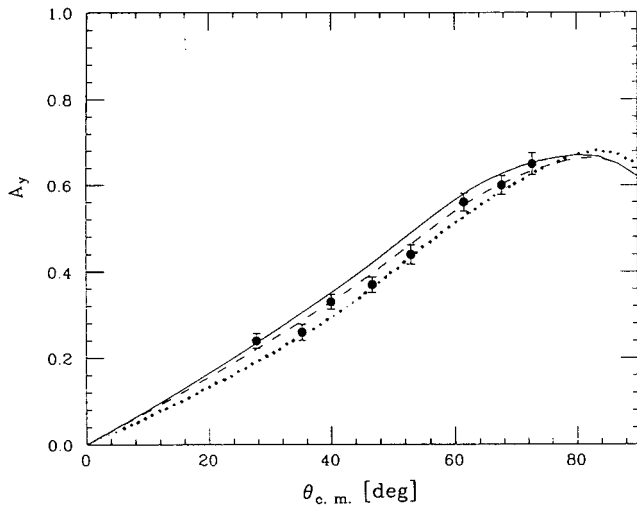


FIG. 8. The analyzing powers for pion charge exchange at 161 MeV [13] are compared to curves for calculations using the three forms of the phase shifts considered in this work. The meanings of the curves are the same as in Fig. 1.

plitudes. The SAID computations and the present results agree with the data of Ref. [8], while the RSL result is far from adequate. Also shown in Fig. 3 are the  $0^\circ$  data for isobaric analog pion charge exchange on  $^{14}\text{C}$ , divided by two, from Ref. [9]. It is evident that the distinctive minimum found in free space is also present for the reaction on the complex target, at much the same laboratory beam energy.

An extensive data set for elastic  $\pi$ -proton scattering at low energies is available near 68 MeV. In Fig. 4 we show the 68.6 MeV data for both pion signs [10]. There are no significant differences between the new results and those of RSL for negative pions at 68.6 MeV, and the present calculations agree well with data at this energy. This is unexpected, since no negative pion data could be included in the fits of RSL. The 68.6 MeV  $\pi^+$  data do not agree at back angles with computations using the parameters of RSL. The 66.8 MeV data of Brack *et al.* [11] are also shown in Fig. 4. The  $\pi^-$  data at these two similar energies agree closely, but the  $\pi^+$  data do not agree at large angles.

At a very similar energy,  $\pi^+$  proton elastic analyzing power data calculations are shown in Fig. 5. It is somewhat unexpected that this observable, so sensitive to interferences, is so much the same using all three phase shift sets.

Near the 3-3 resonance, the fitting effort of RSL was tied to a fairly large data set. It is therefore quite surprising to see how different the cross sections computed from their phase shifts are from the data [12] and from computations using the new phase shift parameters at 141 MeV. A comparison is shown in Fig. 6. Directly at resonance and closely above, all three phase shift forms give agreement with the elastic data of Ref. [12], as shown in Fig. 7.

Another result near resonance is shown in Fig. 8, for the analyzing power in charge exchange [13]. As was the case for elastic analyzing powers at 68 MeV, all three forms of the isovector interaction at 161 MeV are in close concord with one another and, here, with the charge exchange data.

At higher energies, the three forms for the phase shifts

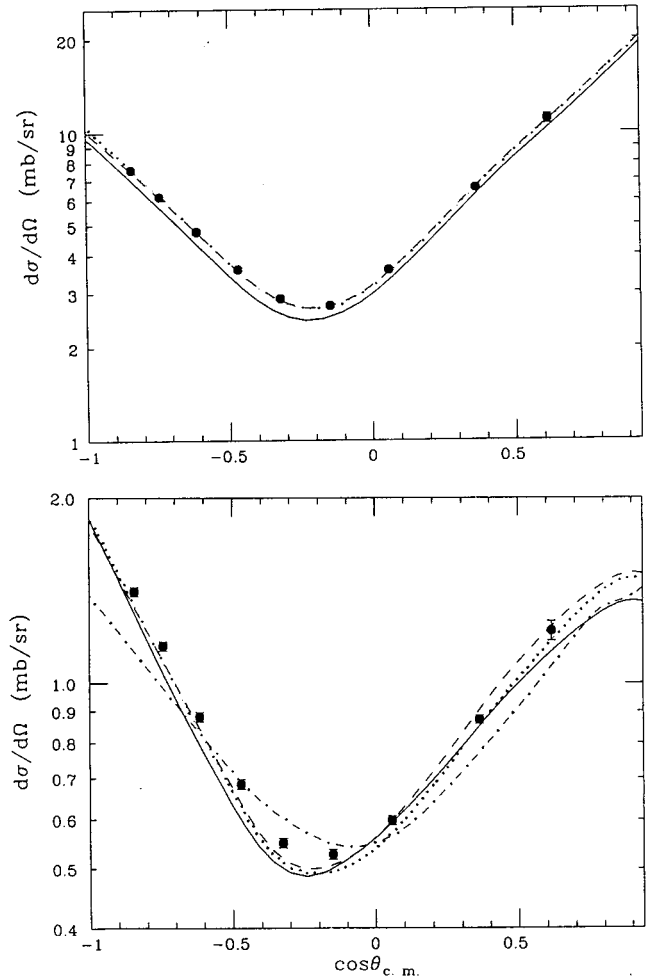


FIG. 9. Data and calculations for elastic scattering from protons are shown for a beam energy of 263 MeV, using data from [14]. The curves have the same meaning as in Fig. 1, and the dot-dashed curve is added to show the effect of deleting the  $D_{13}$  and  $D_{15}$  phase shifts from those provided by the present work. Above are  $\pi^+$  results, with  $\pi^-$  below.

also give agreement with the 263 MeV elastic scattering data of Ref. [14], as shown in Fig. 9. Also shown in Fig. 9(b) are the calculated elastic  $\pi^-$  cross sections from the new parametrization omitting the  $D_{13}$  and  $D_{15}$  waves, but with the other coefficients unchanged. Since it is difficult to include  $D$  and higher waves in pion-nucleus optical model codes, they are often simply omitted. This omission is not relevant for  $\pi^+$ -proton scattering, where only  $T=3/2$  waves are active. The comparison for  $\pi^-$  scattering in Fig. 9 shows this omission of  $D$  waves to have a large effect, destroying agreement with the  $\pi^-$  elastic data at 263.4 MeV.

Pion charge exchange data are shown in Fig. 10 at two energies, compared to computed curves using the three sets of phase shifts [15]. At 128.5 MeV the dotted RSL curve is far from agreement with the data and the other two curves, but all three forms give agreement with the data at 184.8 MeV.

We may conclude this section with the observation that the large and reliable body of  $\pi$ -nucleon data available since the work of Rowe, Salomon, and Landau has indeed made a significant change in their parametrization, and that inad-

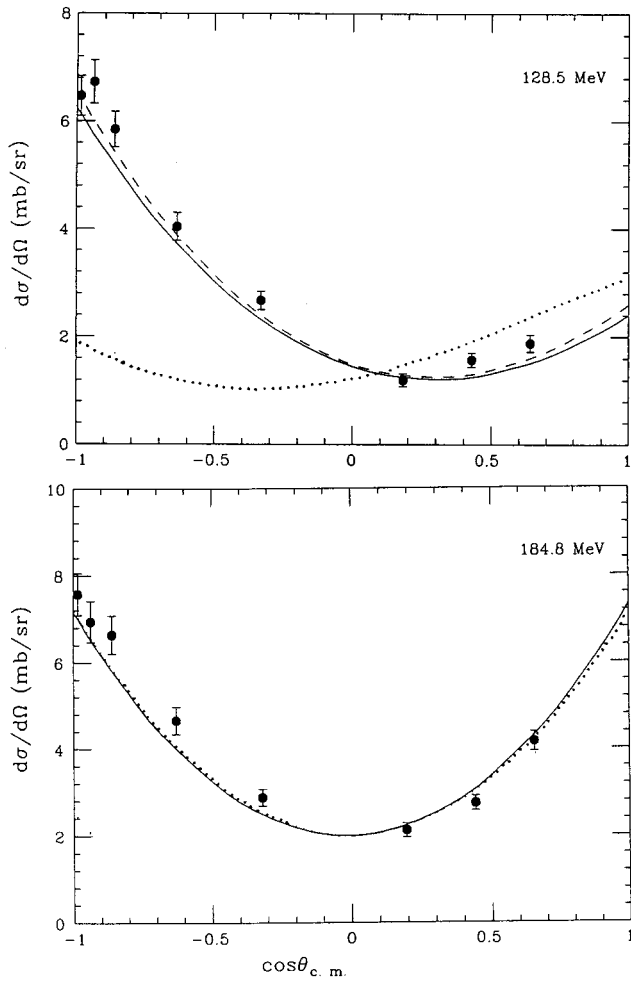


FIG. 10. Charge exchange data on free protons at 128.5 (above) and 184.8 MeV (below) [15] are compared to the three curves using the phase shifts considered in this work, with the same meanings as in Fig. 1.

equacies of that older parametrization are important for some cases of pion-nucleon scattering observables. Especially just below the resonance, the RSL parameters gave poor agreement with recent elastic data at 141 MeV [12] and with charge exchange data at 128.5 MeV [15]. At other energies the results of RSL give observables in agreement with recent data.

### III. EFFECTS ON $\pi$ -NUCLEUS CALCULATIONS

We have modified the first order pion-nucleus distorted wave impulse approximation code DWPI [2] and the second order code DWPIES [3] to use the  $S$ - and  $P$  wave pion-nucleon phase shifts from the present work. Many calculations using these codes have used the  $\pi$ -nucleon interaction of RSL, and we here compare calculations based upon the two forms. All calculations use exactly the same methods and parameters, except for that basic interaction.

An overall view of the differences from the two forms can be seen in the total and reaction cross sections, shown in Fig. 11. The sample nucleus is  $^{52}\text{Cr}$ , with parameters for the distribution of protons and neutrons from Ref. [16], as obtained

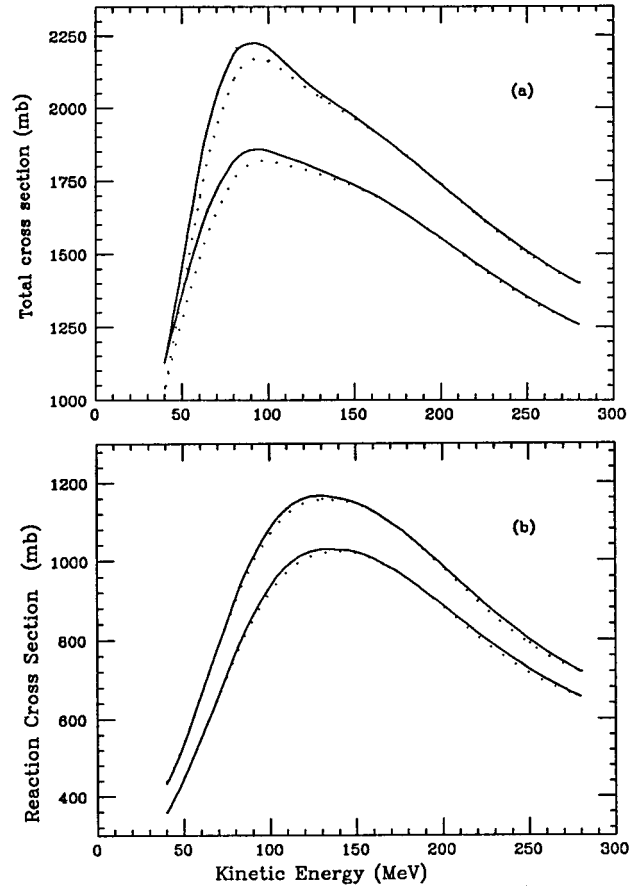


FIG. 11. Total (above) and reaction (below) cross sections for  $^{52}\text{Cr}$  are shown for negative pions as the higher set, and for positive pions as the lower set of curves. Solid lines have used the phase shifts of the present work, and the dotted curves use the phase shifts of RSL, in a first-order optical model calculation.

from fitting pion-nucleus elastic differential cross sections. At high energies, the two  $\pi$ -nucleon forms give very similar results, but differences of 2% are found at resonance and below for the total cross sections. There is less difference between the computed reaction cross sections, indicating that it is the integrated nuclear elastic cross sections that differ significantly.

A first order impulse approximation calculation using the form of RSL has been used for analyses of a large body of inelastic pion-nucleus scattering to discrete states in order to measure the transition matrix elements. These experiments were carried out at the resonance energy in order to optimize the isospin sensitivity to the difference between the  $\pi$ -nucleon channels. A summary and comparison of these results can be found in Ref. [17]. Several of these cases were reexamined using the code DWPI, with all parameters exactly the same, except for the form of the  $\pi$ -nucleon phase shifts. Inelastic differential cross sections computed with a given set of transition matrix elements are the same for the two forms to within 1%. Shapes of computed angular distributions also showed no significant difference using the new or the RSL parameters. The conclusions reached from this large experimental program to determine nuclear transition matrix elements by resonant inelastic pion scattering thus have the

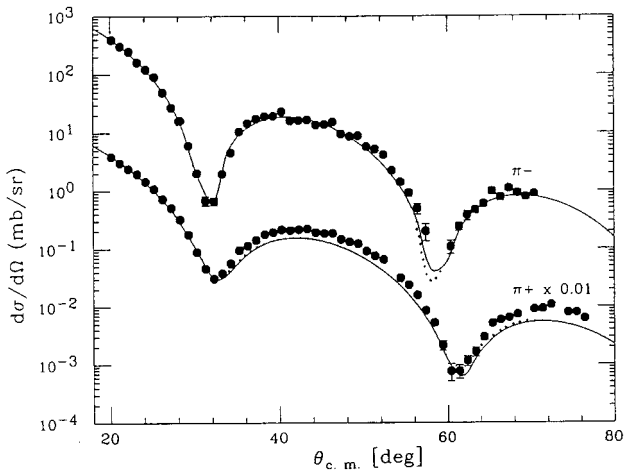


FIG. 12. Data for elastic scattering of 180 MeV negative pions on  $^{42}\text{Ca}$  [18] are compared to DWIA calculations using the phase shifts from the present work as the solid curves and those using the RSL phase shifts as the dotted curve. Also shown are the data and calculations for positive pions, divided by 100.

same validity using either form of the  $\pi$ -nucleon interaction.

The most detailed studies of pion-nucleus interactions come from elastic scattering. It must be remarked here that the normalization scale for the pion-nucleus scattering experiments were often derived from measurements of  $\pi$ -proton scattering in the same spectrometer, and that those  $\pi$ -proton scattering cross sections were often those derived from the work of RSL. There was thus likely to be some desensitizing compensation when those RSL cross sections were also used for the optical model calculations compared to the data. We did not renormalize the published data in light of the newer  $\pi$ -proton cross sections.

We show in Fig. 12 elastic cross sections for pion elastic scattering on  $^{42}\text{Ca}$  at 180 MeV, from Ref. [18]. Parameters are those of that work, where the geometrical distributions of the nucleons in  $^{42}\text{Ca}$  were adjusted until the data were fit. Elastic cross sections computed with the two phase shifts are essentially identical. This was also found to be the case for many other computations of elastic scattering near resonance.

At 292 MeV, where more partial waves are required, calculations of elastic scattering with both pion signs were compared for targets of  $^{40}\text{Ca}$  and  $^{48}\text{Ca}$ , as in the work of [18]. Results are compared in Fig. 13, where no energy shift was used for the present computations. The two sets of calculations are very close, but not in agreement with the data, in the same way that was noted originally [18].

At lower pion beam energies we compare in Fig. 14 the elastic and the inelastic scattering to the first  $2^+$  state of  $^{12}\text{C}$  computed in first order with the RSL and with the new phase shifts, using the code DWPIES [3]. Parameters for the density distribution of  $^{12}\text{C}$  were taken to be those of Ref. [19]. The two curves are in close agreement for both elastic and inelastic scattering, but not like the data [20]; it is known that second order effects are very important at low energies.

In Ref. [19] the second order parameters were used to match the elastic scattering for 50 MeV pions on carbon. These parameters were used in the calculations with both the

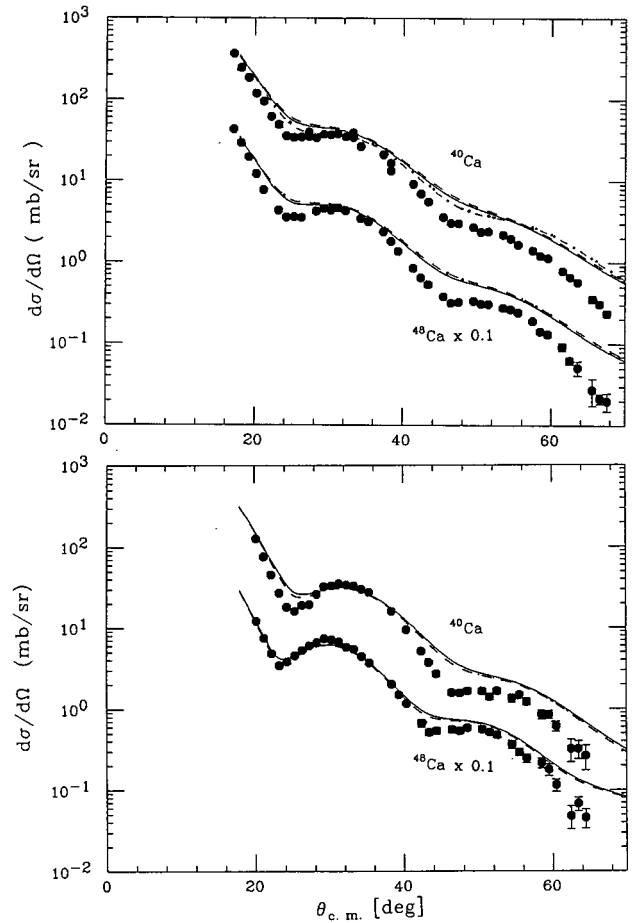


FIG. 13. Above are shown data [18] and calculations for the elastic scattering of 292 MeV positive pions from  $^{40}\text{Ca}$  and from  $^{48}\text{Ca}$ , after division by ten. Solid curves use the phase shifts from the present work, and dotted curves show the results using the phase shifts of RSL. Below are shown the corresponding data and calculations for negative pions. In the comparison to  $\pi^+$  scattering from  $^{40}\text{Ca}$ , the dot-dashed curve uses an optical model formulation much different from that for the solid and dotted curves. See the text.

present and the RSL phase shifts to compute the two very similar curves in Fig. 14(a) that nearly match the elastic data.

Inelastic scattering to the  $2^+$  state at 4.4 MeV was calculated using a derivative transition density and the parameters of [19], with a deformation  $\beta = 0.61$ . The purely first-order calculations are far from the data, but fairly reasonable agreement is found when second order terms are included in calculations using either of the two phase shifts. These sensitivities to second order parameters have been addressed more generally at 50 MeV [21]; what is new here is the comparison of calculations identical except for the choice of the free space  $\pi$ -nucleon phase shifts.

The elastic scattering of 30 MeV  $\pi^+$  from  $^{208}\text{Pb}$  at 30 MeV is strongly influenced by Coulomb scattering, which will interfere with the nuclear scattering calculated with the two sets of phase shifts. We show in Fig. 15 the data [22] compared to DWPIES calculations using the present phase shifts and those of RSL. The second order parameters were taken to be exactly those used for  $^{12}\text{C}$  in Ref. [19]. Our point is not to fit the data for each case, but to show the influence

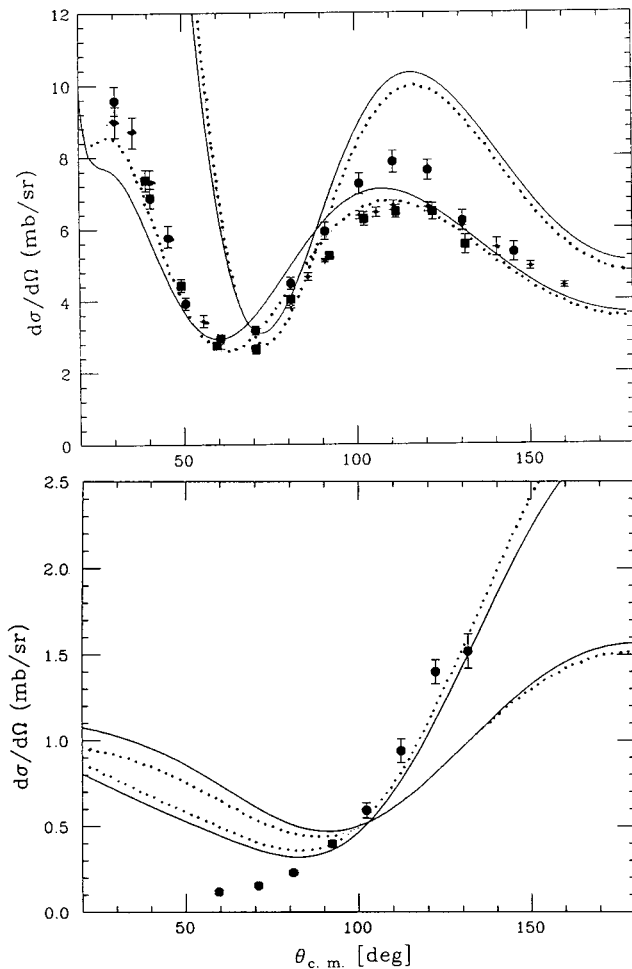


FIG. 14. Above are shown elastic  $\pi^+$  data near 50 MeV for a carbon target [20]. Optical model calculations from the DWIA code DWPIES [3] are shown using the phase shifts from the present work for the solid curves and phase shifts from RSL for the dotted curves. The two curves sitting above the data are for first order calculations, while the two curves nearly in agreement with the data use the second order terms of [19]. Below are shown the data [20] and DWIA calculations for  $\pi^+$  scattering to the 4.4 MeV  $2^+$  state of  $^{12}\text{C}$ , with the first order calculations falling below the large angle data, and the calculations including second order terms nearly matching the large angle data.

of the choice of  $\pi$ - $N$  phase shifts. The difference for  $^{208}\text{Pb}$  is not great, but the present phase shifts do give quite good agreement with the elastic data.

Pion single charge exchange calculations on complex nuclei use the isovector amplitudes only, in contrast to the primarily isoscalar amplitudes examined by scattering. Our test case is the  $^{14}\text{C}(\pi^+, \pi^0)^{14}\text{N}$  reaction leading to the isobaric analog  $0^+$  state at 2.31 MeV. This reaction proceeds only through an  $L=0$  angular momentum transfer. The middle panel of Fig. 16 shows first-order distorted-wave impulse approximation (DWIA) calculations for this transition at 164.5 MeV, using both the RSL amplitudes and those from the present work. Geometrical parameters are those of Ref. [19], designed for  $^{12}\text{C}$ , but applied here to  $^{14}\text{C}$  for purposes of comparison. The transition density shape is taken to be the

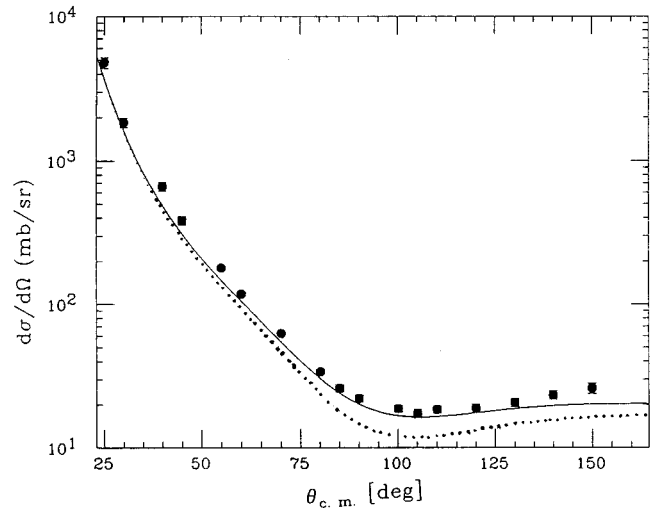


FIG. 15. Data for elastic scattering of 30 MeV positive pions from  $^{208}\text{Pb}$  [22] are compared to DWIA calculations using phase shifts from the present work for the solid curves and the phase shifts of RSL for the dotted curves. The second order optical model terms are those used for  $^{12}\text{C}$  in Ref. [19].

first derivative of the ground state distribution, and the reaction model is that of Ref. [3], using the code DWPIES. It is evident that there is essentially no difference between the results using the two phase shift forms. Also shown for comparison are the data from Ref. [9].

A greater sensitivity to the choice of phase shift forms is found at 50 MeV, as shown in the top panel of Fig. 16. Geometrical parameters and second order parameters are taken from the fits at 50 MeV [19]. Differences between the two computed shapes are small, however, compared to the difference each has from the data shown [9]. The source of the failure to match the data does not arise from the choice of the  $\pi$ -nucleon data set.

In the bottom panel of Fig. 16 we show first order DWPIES calculations for the IAS transition from  $^{14}\text{C}$  with the same geometrical parameters, at 246 MeV. At small angles the results from the use of RSL amplitudes are significantly below those using the present phase shifts. As for the other examples computed in the DWIA, no  $D$  waves are included in the  $^{14}\text{C}$  calculations shown in Fig. 16.

#### IV. DISCUSSION AND CONCLUSIONS

We have used the idea and the parametrization of Rowe, Salomon, and Landau [1] for a new fit to pion-nucleon interactions from 30 – 300 MeV of pion kinetic energy. We used more modern resonance terms, and we searched the terms in the parametrized expression of RSL to fit a consistent set of phase shifts determined by a recent analysis of a wide body of  $\pi$ -proton observables [4]. Since our starting parameters were taken to be the final results of RSL, the same fitting minimum is retained.

Overall, the phase shifts from RSL, which preceded most of the data now accepted, are found to be very similar to the modern results. Calculations using the present set of phase shifts, as listed in Table I, have been shown to match experi-



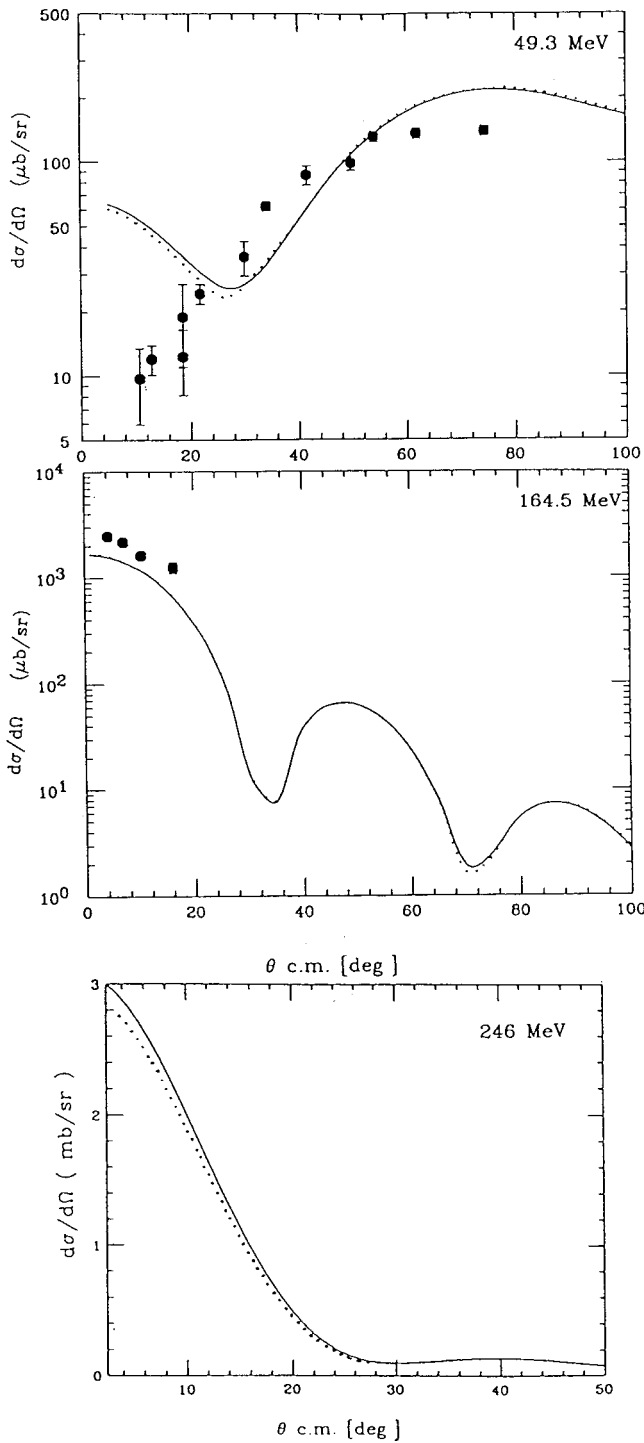


FIG. 16. Calculations from the DWIA code DWPIES [3] are shown for the isobaric analog transition in the  $^{14}\text{C}(\pi^+, \pi^0)^{14}\text{N}$  reaction, using phase shifts from the present work for the solid curves and using the RSL phase shifts for the dotted curves. The top portion is for a beam energy of 49.3 MeV, and uses the geometrical and the second-order parameters of Ref. [19]. Data are from Ref. [9]. The middle portion is for 164 MeV, with data from [9]. The lower portion is for 246 MeV.

mental  $\pi$ -proton observables very well in all cases. Many more cases than presented here were examined.

The greatest inability of the RSL phase shifts to account for data was found for charge exchange. This is not surprising, since no charge exchange data were available to those

authors. The sharp minimum in the  $0^\circ$  charge exchange cross section near 46 MeV is badly missed in the calculations based on the RSL results, but matched with the present form. See Fig. 3. Also, at 128.5 MeV the RSL charge exchange calculations are greatly different from the data.

The only significant difference between the RSL and the present computations for elastic  $\pi$ -proton scattering was found at 141 MeV, shown in Fig. 6. Use of the present phase shifts gives good agreement with recent data. At 168.8 MeV, the two calculations agree, as shown in Fig. 7.

When the present parametrization is used in the DWIA codes DWPI [2], in first order only, or in DWPIES [3], in both first and second order, we found very little difference between the total or the reaction cross sections from calculations using the RSL values. Elastic scattering calculations using either set of phase shifts near the resonance energy were found to be nearly indistinguishable, as shown in Fig. 12. This was also found to be true for a wide range of inelastic scattering calculations, such that transition matrix elements determined by resonance energy pion scattering are secure. These two satisfying agreements are undoubtedly due to the fact that at resonance the  $\pi$ -nucleon cross sections are so large that the scattering is essentially that from a black disk, and the details are not important.

Pion-nucleus elastic scattering at high energies is generally computed in the DWIA without including the  $D$  waves. We showed in Fig. 9 that this neglect spoils agreement with  $\pi$ -proton data. To study the effect of the lack of  $D$  and higher waves for  $\pi$ -nucleus scattering, we show in Fig. 13(a) a dot-dashed curve for  $^{40}\text{Ca}$  computed with the optical model code of Chen *et al.* [23], based upon the eikonal approximation, and including all partial waves. A Fermi-averaging procedure is used for the proper evaluation of the partial waves within the complex nuclear target. The geometrical parameters for  $^{40}\text{Ca}$  were the same as those used for the dotted and the solid curves using DWPI. It is seen in Fig. 13(a) that the inclusion of a complete set of partial waves makes almost no difference to the computed cross sections.

Low pion beam energies find a rather transparent nucleus, and their scattering is known to be sensitive to the reaction parameters. It is also at low pion energies that the data base for the free scattering has changed the most since the work of RSL. Nonetheless, the differences between first- or second order calculations using the RSL or the present phase shifts were found to be slight. We examined this for 50 MeV elastic and inelastic scattering on  $^{12}\text{C}$  and for 30.7 MeV elastic scattering from  $^{208}\text{Pb}$ . Even for pion charge exchange, differences between DWIA calculations with the two families of phase shifts differ little at any energy. No major reconsiderations of the role of the interesting second order parameters is required, and the important conclusions drawn from these studies remain valid.

It was pointed out long ago that a firm foundation of  $\pi$ -nucleon interactions is required for reliable DWIA calculations of  $\pi$ -nucleus scattering [24]. A great investment in analyzing  $\pi$ -nucleus data relied heavily on the parameters of RSL, with little consideration of changes in the data base of  $\pi$ -nucleon scattering. This dangerous situation has been remedied by the present work, and future DWIA computations

for 30–300 MeV can be very certain of a reliable connection to free scattering. It is fortunate and satisfying that  $\pi$ -nucleus calculations as commonly carried out have now been shown to have been quite nearly correct when using the RSL parameters.

#### ACKNOWLEDGMENTS

We wish to thank D. Prull for help in the fitting routines, and Assiut University for support of this work, which was also supported in part by the U.S. DOE.

- 
- [1] G. Rowe, M. Salomon, and R. H. Landau, *Phys. Rev. C* **18**, 584 (1978).
  - [2] R. A. Eisenstein and G. A. Miller, *Comput. Phys. Commun.* **11**, 95 (1976).
  - [3] M. B. Johnson, *Phys. Rev. C* **22**, 192 (1980); M. B. Johnson and E. R. Siciliano, *ibid.* **27**, 1647 (1983).
  - [4] R. A. Arndt, I. I. Strakovsky, R. L. Workman, and M. M. Pavan, *Phys. Rev. C* **52**, 2120 (1995).
  - [5]  *$\pi$ -N Newsletter*, edited by G. Höhler, W. Kluge, and B. M. K. Nefkens (Universitätsdruckerci, Universität Karlsruhe, 1995).
  - [6] Particle Data Group, L. Montanet *et al.*, *Phys. Rev. D* **50**, 1173 (1994).
  - [7] M. E. Sadler, private communication.
  - [8] D. H. Fitzgerald *et al.*, *Phys. Rev. C* **34**, 619 (1986).
  - [9] J. L. Ullmann *et al.*, *Phys. Rev. C* **33**, 2092 (1986).
  - [10] C. Joram *et al.*, *Phys. Rev. C* **51**, 2159 (1995).
  - [11] J. T. Brack *et al.*, *Phys. Rev. C* **41**, 2202 (1990).
  - [12] M. M. Pavan, Ph.D. thesis, University of British Columbia (unpublished).
  - [13] J. J. Görge *et al.*, *Phys. Rev. D* **42**, 2374 (1990).
  - [14] M. E. Sadler, W. J. Briscoe, D. H. Fitzgerald, B. M. K. Nefkens, and C. J. Seftor, *Phys. Rev. D* **35**, 2718 (1987).
  - [15] R. F. Jenefsky, C. Joseph, M. T. Tran, B. Vaucher, E. Winkelmann, T. Bressani, E. Chiavassa, G. Venturullo, H. Schmitt, and C. Zuparcic, *Nucl. Phys.* **A290**, 407 (1977).
  - [16] D. S. Oakley *et al.*, *Phys. Rev. C* **35**, 1392 (1987).
  - [17] R. J. Peterson, *Phys. Rev. C* **48**, 1128 (1993).
  - [18] K. G. Boyer *et al.*, *Phys. Rev. C* **29**, 182 (1984); K. G. Boyer, Los Alamos Report No. LA-9974-T, 1984.
  - [19] R. Alvarez del Castillo and N.B. deTakacsy, *Phys. Rev. C* **43**, 1389 (1991).
  - [20] R. J. Sobie *et al.*, *Phys. Rev. C* **30**, 1612 (1984), and references therein.
  - [21] J. A. Carr, H. McManus, and K. Stricker-Bauer, *Phys. Rev. C* **25**, 952 (1982).
  - [22] B. M. Freedom *et al.*, *Phys. Rev. C* **23**, 1134 (1981).
  - [23] C. M. Chen, D. J. Ernst, and M. B. Johnson, *Phys. Rev. C* **48**, 841 (1993).
  - [24] R. H. Landau and A. W. Thomas, *Phys. Lett.* **61B**, 361 (1976).